Initial laboratory experiments to validate a phase and amplitude gradient estimator method for the calculation of acoustic intensity

Darren K. Torrie, Eric B. Whiting, Kent L. Gee, Traciannne B. Neilsen, and Scott D. Sommerfeldt

Citation: Proc. Mtgs. Acoust. **23**, 030005 (2015); doi: 10.1121/2.0000348
View online: http://dx.doi.org/10.1121/2.0000348
View Table of Contents: http://asa.scitation.org/toc/pma/23/1
Published by the Acoustical Society of America

Proceedings of Meetings on Acoustics

Volume 23 http://acousticalsociety.org/

169th Meeting of the Acoustical Society of America

Pittsburgh, Pennsylvania

18-22 May 2015

Engineering Acoustics: Paper 4pEA5

Initial laboratory experiments to validate a phase and amplitude gradient estimator method for the calculation of acoustic intensity

Darren K. Torrie, Eric B. Whiting, Kent L. Gee, Traciannne B. Neilsen, and Scott D. Sommerfeldt

Department of Physics and Astronomy, Brigham Young University, Provo,Utah;darren@torriefamily.org, benweric@gmail.com, kentgee@byu.edu, tbn@byu.edu, scott_sommerfeldt@byu.edu.

A recently developed phase and amplitude gradient estimator (PAGE) method for calculating acoustic intensity from multiple pressure measurements [Thomas et al., J. Acoust. Soc. Am. 137, 3366 (2015)] has been tested via anechoic laboratory measurements of the radiation from broadband sources. The measurements determine that the effective frequency bandwidth of valid acoustic intensity calculations can be substantially increased when using the PAGE method over the traditional cross-spectral approaches. Preliminary results are shown for two probe sizes and multiple broadband source configurations.

Published by the Acoustical Society of America

 [DOI: 10.1121/2.0000348]

1. INTRODUCTION

Anechoic laboratory experiments were conducted to validate the recently developed phase and amplitude gradient estimator[1] (PAGE) method in a controlled environment. The PAGE method was originally developed to maximize the useable bandwidth of active, acoustic vector intensity measurements in rocket noise source characterization in outdoor settings.[2] The PAGE method has also been applied to measure acoustic intensity near military aircraft[3] and laboratory-scale jets.[4] The results of anechoic laboratory experiments indicate that, in general, the PAGE method extends the usable bandwidth of acoustic intensity relative to traditional calculation procedures, but care must be taken if deep interference nulls are present in the acoustic field.

The standard p-p method for active acoustic intensity, which will be referred to as the traditional method, involves taking finite sums and differences of the complex pressure between pairs of microphones that, when ensemble averaged, involve weighted quadspectra.[5] The traditional method has been used for source modeling and localization in both engineering and research applications.[6] As the microphone spacing becomes comparable to the wavelengths of the incident waves, spatial aliasing causes bias errors in the estimated pressure and particle velocity required for the intensity calculation.[7] This limitation[8] has been sufficiently studied,[9] the appropriate bandwidth has been defined for a given microphone spacing, and has been included in many standards.[10,11] The PAGE method uses the amplitude and phase components of the complex pressures, which typically vary more linearly across the microphone pair than the real and imaginary parts.[12] Both the theory and initial implementations of the PAGE method indicate robustness that extends the usable bandwidth of active intensity calculations.

2. BACKGROUND

2.1 Two-dimensional Intensity Probe

Each measurement in the anechoic laboratory experiments was taken using a two-dimensional intensity probe configuration developed for rocket noise measurements.[13] For the laboratory measurements, the probe consists of four, coplanar, 6.35mm diameter, GRAS 40BD pressure microphones, shown in Figure 1. The chosen probe geometry forms an equilateral triangle with microphone A at the probe center of mass, and microphones B, C, and D located at a radius a. The x-y position of each microphone, relative to the center microphone, can be expressed as

$$\boldsymbol{r_A} = \begin{bmatrix}0\\0\end{bmatrix}, \quad \boldsymbol{r_B} = a\begin{bmatrix}0\\-1\end{bmatrix}, \boldsymbol{r_C} = \frac{a}{2}\begin{bmatrix}\sqrt{3}\\1\end{bmatrix}, \boldsymbol{r_D} = -\frac{a}{2}\begin{bmatrix}\sqrt{3}\\-1\end{bmatrix}. \quad [1]$$

Two sizes of intensity probe, $a = 2.54$ and 5.08 cm, are used in the measurements.

Figure 1 *- Two-dimensional, four-microphone intensity probe schematic (left) and photograph (center) with specific radius* $\boldsymbol{a}$ *= 5 cm containing four 6.35mm diameter GRAS 40BD pressure microphones. (Right) Photograph of the experimental setup in the large anechoic chamber at BYU with an intensity probe attached upside down to the movable boom arm in front of a box of loudspeakers.*

2.2 Methods

The traditional p-p method for calculating the radiated or active intensity directly uses either a directly measured or average pressure at the probe center and an estimate of the acoustic particle velocity found by using a finite difference approach to Euler's equation.[14] The estimated active intensity, $\hat{I}^{\mathrm{TRAD}}$, in the frequency domain is

$$\hat{\boldsymbol{I}}^{\mathrm{TRAD}} = \frac{1}{\rho_0 \omega} p_0 \widehat{\boldsymbol{\nabla p}}^{*}, \qquad [2]$$

where ω is the angular frequency, ρ_0 is the density of air, the average pressure, p_0, is the pressure estimated or measured at the center of the intensity probe halfway, and $\widehat{\boldsymbol{\nabla p}}^{*}$ is the conjugate of the estimated complex pressure gradient estimated.

In practice, this yields a cross-spectral analysis of pressure measurements between multiple phase-matched microphones. In the case of the four-microphone intensity probe used in this study (see Figure 1), the x and y components of the traditional, active intensity estimations can be represented in matrix form:

$$\hat{\boldsymbol{I}}^{\boldsymbol{TRAD}} = \frac{1}{6\rho_0 \omega a}\begin{bmatrix} \sqrt{3}\, \boldsymbol{Im}\{\boldsymbol{G_{CA}} - \boldsymbol{G_{DA}}\} \\ 2\, \boldsymbol{Im}\{\boldsymbol{G_{BA}} - \boldsymbol{G_{CA}} - \boldsymbol{G_{DA}}\} \end{bmatrix}, \qquad [3]$$

where $G_{ij} = \langle 2p_i^* p_j \rangle$ is the time-averaged, single-sided cross-spectrum between the complex pressure p at microphones i and j.

The accuracy of the gradient estimation in the intensity calculation is vital to obtaining quality results. There are two common sources of error in the estimated gradient: bias errors that eventually give way to spatial aliasing at high frequencies and microphone phase mismatch at low frequencies.[15] These errors are both related to the size of the acoustic wavelength relative to the spacing between microphones. First, when the wavelength becomes small relative to the microphone spacing, the gradient is undersampled which introduces errors into the estimation. When the wavelength is large relative to the microphone spacing, the difference in the phase of the wave received at the two microphones is relatively small and can be comparable to the phase mismatch between the microphones. The need for closely spaced microphones to reliably estimate intensity at high frequencies competes with the need to have the microphones spaced farther apart to get reliable intensity at lower frequencies. These two limitations cause traditional p-p intensity

estimates to be appreciably band limited. The PAGE method helps to address both of these limitations, thereby increasing the usable bandwidth of intensity estimates.

The PAGE method was developed at BYU in conjunction with models of high intensity broadband sources that includes solid rocket motors,[2] military aircraft[3] and laboratory-scale jets.[4] The PAGE method estimates the acoustic intensity by manipulating Equation 2 based on the amplitude and phase components of the complex pressures, $p = Pe^{j\phi}$, of the multiple phase-matched microphones. The active acoustic intensity is now written as

$$\hat{\boldsymbol{I}}^{\boldsymbol{PAGE}} = \frac{\mathbf{1}}{\boldsymbol{\omega\rho_0}} \boldsymbol{P^2 \nabla \varphi}, \quad [4]$$

where P is the pressure amplitude at the center of the intensity probe, and φ is the relative phase across the microphone pairs. For the given probe configuration shown on the right hand side of Figure 1 the x and y components of the active intensity estimations are

$$\hat{\boldsymbol{I}}^{\boldsymbol{PAGE}} = \frac{G_{AA}}{6\omega\rho_0 a}\begin{bmatrix} \sqrt{3}\boldsymbol{arg}\{\boldsymbol{H_{CD}}\} \\ \boldsymbol{arg}\{\boldsymbol{H_{BC}}\} + \boldsymbol{arg}\{\boldsymbol{H_{BD}}\} \end{bmatrix}. \quad [5]$$

In Equation 5, G_{AA} is the autospectrum of the center microphone, and $\arg\{H_{ij}\}$ represents the argument (or phase) of the complex transfer function between microphones i and j. In a propagating wave field, the PAGE amplitude estimation is relatively simple because the amplitude is smoothly varying. The gradient of the phase, however, is a discontinuous function that alternates between ±π. An unwrapping algorithm can be applied to this phase component of the pressure so that it becomes a continuous function. This allows for a reliable gradient of the phase to be obtained beyond the spatial Nyquist frequency, f_N, so long as the unwrapping functions properly. For this work, the basic unwrapping algorithm in MATLAB is used, but improved unwrapping techniques are under investigation.

2.3 Experiment

The experiments were conducted in BYU's large anechoic chamber, which has working dimensions of 8.71 m by 5.66 m by 5.74 m and a frequency range of 80 - 20,000 Hz. This chamber is equipped with a precision three-dimensional positioning system allowing an intensity probe to be positioned anywhere in the chamber. For these experiments, the scan configuration is limited to movement only in the horizontal (x-y) plane of the chamber.

The sources were the middle two elements of a loudspeaker array consisting of four 6.3 cm loudspeakers with an element spacing of 17.78 cm. The two-dimensional intensity probe in Figure 1 was mounted to the scanning system and positioned such that the plane of the probe was parallel to the floor and set at the height of the middle of the loudspeakers array. The x-axis is parallel to the front face of the speaker array, and the y-axis comes out perpendicular from the front face of the speaker array.

The origin of the x-y plane was in between the two speakers in the x-direction for a two source configuration and at the center of one of the speakers for the single source case. This places the speakers themselves directly along the x-axis. Due to the probe size, measurements actually start 7.62 cm from the surface of the speaker box. A centered 1 m by 1 m grid of 41 points by 41 points (1681 measurement positions) was defined in the x-y plane in front of the loudspeaker array, with a resolution of 5 cm in each direction. Each location corresponds to a measured intensity vector. The record length at each measurement position is 10 s, such that each scan took approximately 9 hours to complete.

Several source-probe configurations were measured: 1.) A single loudspeaker radiating broadband white noise measured using the $a = 5.08$ cm probe; 2.) Two loudspeakers broadcasting out-of-phase broadband white-noise signals measured using the $a = 5.08$ cm probe; 3.) Two loudspeakers generating different broadband white-noise signals measured using the $a = 5.08$ cm probe; and 4.) Two loudspeakers producing different broadband white-noise signals measured using the $a = 2.54$ cm probe. These results were compared to a baffled circular piston model, based on Rayleigh integrals for both acoustic pressure and particle velocity and used to simulate the intensity field from the loudspeakers.[16]

2.4 Models

An analytical model of radiated acoustic vector intensity is important to establishing a benchmark for the laboratory studies, especially at high frequencies beyond the limits of the traditional method. A baffled circular piston model was developed in MATLAB to simulate the intensity field from a broadband noise source[17]. Rayleigh integrals were used to estimate p and $\boldsymbol{u}$ separately at each grid point and the resultant intensity was calculated. Each vector has a scaled magnitude, creating a symmetric vector field relative to each other, as represented by the size of the arrow as well as the color of the plot behind the arrow. The intensity angle is referenced to zero degrees along the positive horizontal axis. An example of the resulting intensity vector field from one such source at 600, 6000, and 12 kHz is shown in Figure 2, to demonstrate how the source propagation changes with frequency and to show frequencies above and below the limitations of the Traditional method if using a probe with 5-cm spacing.

The intensity from a single baffled circular piston is frequency dependent. At 600 Hz (left) the source looks very much like a monopole, but at 6 kHz (middle) the source becomes much more directional. At sufficiently high frequencies, as is evident at 12 kHz (right), there is one main lobe with minor side lobes. These patterns are typical for a baffled circular piston source at high frequencies.

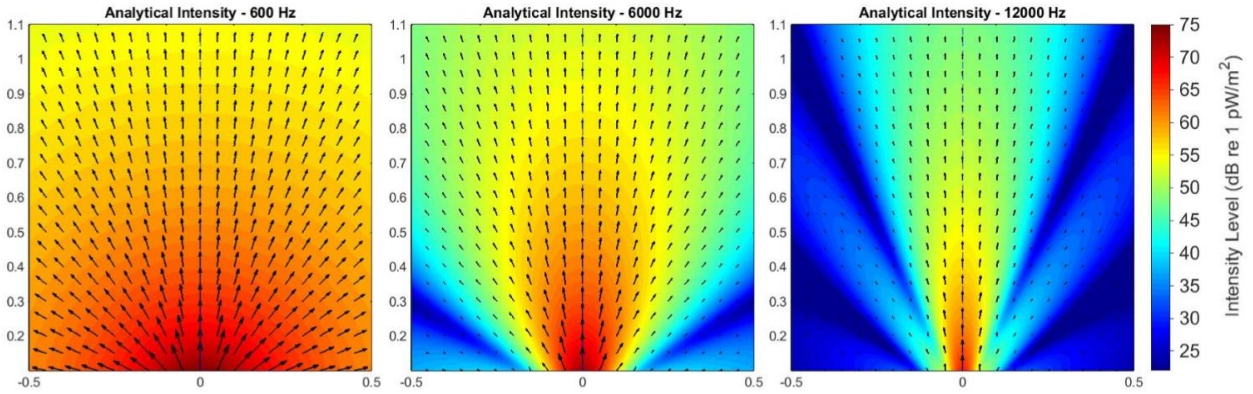

Figure 2 - *A computational simulation of a baffled circular piston radiating a broadband noise signal at 600 Hz (left), 6000 Hz (middle), and 12 kHz (right). The vectors represent the resulting intensity of at each grid point and the color map shows the resulting magnitude of the intensity across the field.*

The model is expanded to incorporate two baffled circular piston sources the same size and strength and that are each emitting the same broadband noise signal 180° out of phase from each other. In this model there are several unique features exhibited as seen in Figure 3. First, an interference null forms directly in between the two sources. Here the intensity effectively goes to zero. This null is present for all frequencies. The radiation formation at 600 Hz (left), is dipole-like, with a solitary null equidistant between the two sources. At 12 kHz (right), there are multiple

interference nulls that form out at various angles from the source. The intensity also drops off on the sides of the source as a result of the source being more directional at 12 kHz (right).

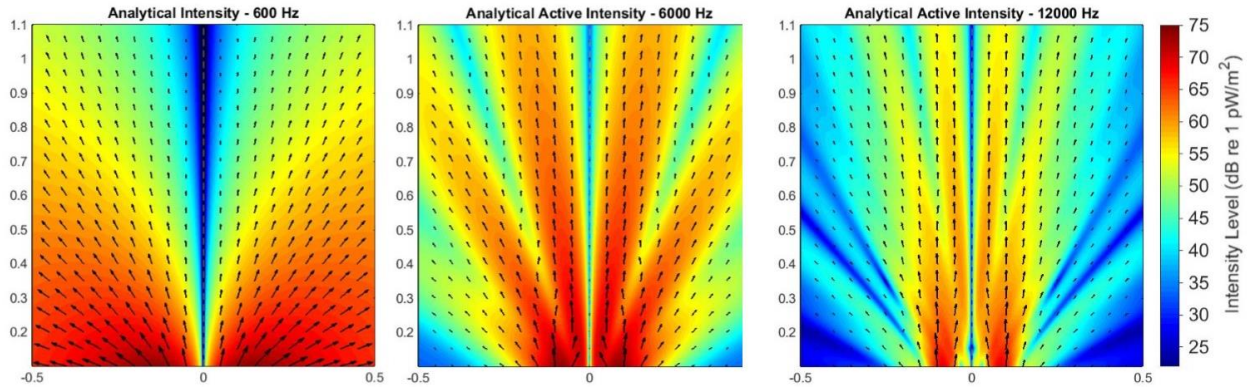

Figure 3 - *A computational simulation of two baffled circular pistons radiating the same broadband noise signal 180 degrees out of phase from each other at 600 Hz (left), 6000 Hz (middle), and 12 kHz (right). The vectors represent the resulting intensity of at each grid point and the color map shows the resulting magnitude of the intensity across the field.*

The third and final model configuration consists of two baffled circular pistons that are each radiating a unique or incoherent broadband signal in Figure 4. This creates an intensity field that looks very comparable to the single source model at 600 Hz (left). At 12 kHz (right), the two sources are more apparent and are radiating independently of each other without causing any interference nulls where the two fields are over lapping.

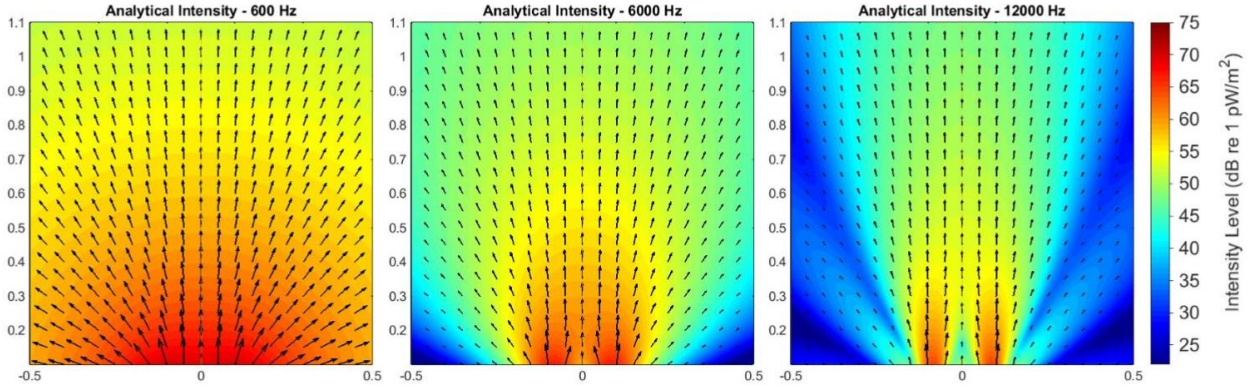

Figure 4 - *A computational simulation of two baffled circular pistons each radiating a unique broadband noise signal at 600 Hz (left), 6000 Hz (middle), and 12 kHz (right). The vectors represent the resulting intensity of at each grid point and the color map shows the resulting magnitude of the intensity across the field.*

The modeled intensity vectors in Figure 2, Figure 3, and Figure 4 provide a ground truth for the laboratory experiments with three different source configurations, as the acoustic intensity vectors should resemble the model for the same designated frequencies.

3. RESULTS AND ANALYSIS

For the purposes of comparing the traditional and PAGE methods with vector plots, only a few frequencies are examined for the source-probe configurations described above. Because it is the relationship between wavelength and probe size that produces the limit of the processing accuracy for the traditional method, each configuration includes vector plots at 600 Hz, below the spatial Nyquist frequency, 6000 Hz, above the spatial Nyquist frequency, and 12 kHz, well above the

spatial Nyquist frequency. (For the 5.08 cm probe, $f_N \approx 2$ kHz, and for the 2.54 cm probe, $f_N \approx 4$ kHz.) Additional results for intensity level and direction are shown as a function of frequency for specific probe locations. These plots give intuition as to the starting frequency of the bias errors for the traditional method and the overall frequency bandwidth of each method, and how the probe configuration and size impacts them. A difference of 1 dB between the calculated intensity level and the measured sound pressure level is used to define when the method is no longer accurate.

3.1 Single Source, 5-cm Probe

The first experiment consisted of an intensity probe, with $a = 5.08$ cm, to measure the sound field of a single loudspeaker radiating broadband noise. The resulting intensity vector plots are displayed in Figure 5 with the traditional method on the left hand side and the PAGE method on the right hand side, at the frequencies of 600 Hz (top), 6 kHz (middle), and 12 kHz (bottom). The y-axis is centered on the loudspeaker. At 600 Hz (top of Figure 5), both methods have intensity fields similar to that of a monopole, radiating out from the speaker in all directions. Both traditional (left) and PAGE (right) are similar to the model of a baffled circular piston in Figure 2. At 6 kHz (middle of Figure 5), the radiation pattern from the loudspeaker begins to become more directional, as seen by the magnitude rolling off on the sides. The traditional method estimate for the active intensity, however, has already deteriorated by this frequency. The arrows are pointing back towards the source, and the magnitudes across the field are all lower than those of the model. On the other hand, the PAGE method still has meaningful energy propagation direction across the field. While the traditional method falls off by this point, the PAGE continues to give results that are comparable to the analytical model. The 12 kHz (bottom of Figure 5) case has several lobes with distinct nulls in the field, as is expected from the analytical model at 12 kHz for a single source shown in Figure 2. Only the PAGE method captures the anticipated behavior. The traditional method results at 12 kHz have incorrect directions and magnitudes that are far too low to be realistic for an actively radiating source.

Although Figure 5 is useful for visualizing the field behavior at specific frequencies, the frequency dependence of the accuracy of the two processing methods is clearest by examining a single measurement location. The magnitude (left) and direction (right) of active intensity vectors at location (-0.15, 0.45) m are shown in Figure 6. The magnitude of the intensity (left) should follow the sound pressure level (SPL) of the center microphone for all frequencies in the case of a propagating wave. The magnitude estimated by the PAGE method follows the SPL closely for all frequencies, whereas the traditional method error exceeds 1 dB at approximately 2 kHz, with increasing error as a function of frequency. As for the direction plot (right) of the intensity in Figure 6, the direction of propagation should be similar for all frequencies. This is true for the PAGE method, which remains constant beyond 12 kHz. The direction of the intensity vector from the traditional method, however, begins to deviate after 3 kHz, eventually resulting in a physically implausible direction.

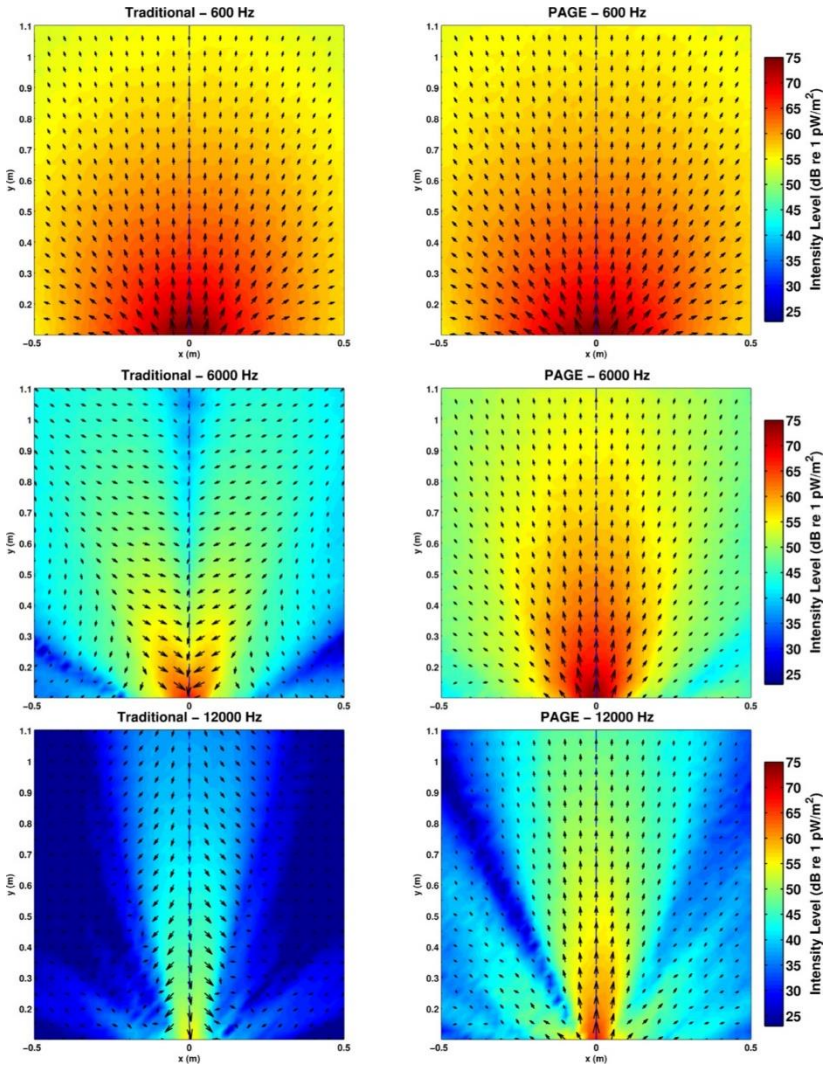

Figure 5 - *Estimates of active intensity from the traditional method (left) and PAGE method (right) at frequencies of 600 Hz (top), 6000 Hz (middle), and 12 kHz (bottom) a two-dimensional probe with radius of 5-cm measuring a single loudspeaker emitting broadband white noise.*

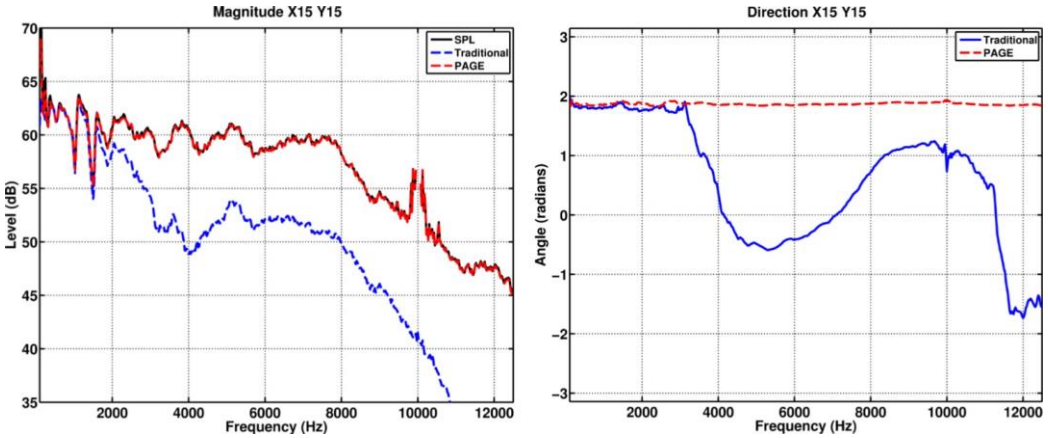

Figure 6 - *The resulting magnitude (left) and direction (right) of the frequency-dependent intensity vector at the spatial location, in meters, of (-0.15, 0.45) for a single loudspeaker radiating broadband white-noise. Measurements taken using a two-dimensional probe with radius of 5-cm.*

3.2 Two Sources Coherent 5-cm Probe

This next set of measurements was taken with a 5.08-cm probe of two loudspeakers radiating broadband noise, 180° out of phase from each other. The corresponding intensity vector plots are displayed in Figure 7 with the traditional method on the left and the PAGE method on the right, at 600 Hz (top), 6 kHz (middle), and 12 kHz (bottom). The y-axis is centered between the two loudspeakers. The spatial maps show the overall performance of the two methods in obtaining the vector intensity sound field. At 600 Hz (top of Figure 7), for both methods the two speakers are obviously radiating outward with an interference null forming directly between the two sources. This null is not as prominent in the measurements near the sources at this frequency, as it is in the analytical model. The null is deeper for the traditional method than for the PAGE method; however, both methods are similar to the model in Figure 3. At 6 kHz (middle of Figure 7), the distinct null between the speakers forms more clearly in the PAGE method, whereas the traditional method has produced nonphysical results. These differences between the PAGE and traditional methods persist at 12 kHz; the PAGE method yields intensity vectors that are representative of the analytical model while the traditional method's results are nonphysical.

The magnitude (left) and direction (right) from the vector at location (-0.15,0.45) m for the coherent two-source case is shown in Figure 7. Similar to the single loudspeaker case, the magnitude plot (left) shows that the PAGE (red) method follows the SPL (black) of the center microphone of the probe very closely all the way up to 12 kHz. The dip in both the SPL and the PAGE method are due to the formation of a null at the probe's location that reaches its minimum at just above 6 kHz. The traditional method (blue) begins to roll off and has a difference of greater than 1 dB at 2 kHz and continues to drop off as the frequency increases. The direction (right) of the intensity at this location, and in this source configuration is expected to remain unchanged for most frequencies except for in the presence of a null that occurs around 6 kHz. The PAGE method (red) remains unchanged up to 12 kHz, with only a slight variation through the null at 6 kHz. The traditional method (blue) however begins to differ again before 3 kHz and never recovers, leaving the direction to be unreliable.

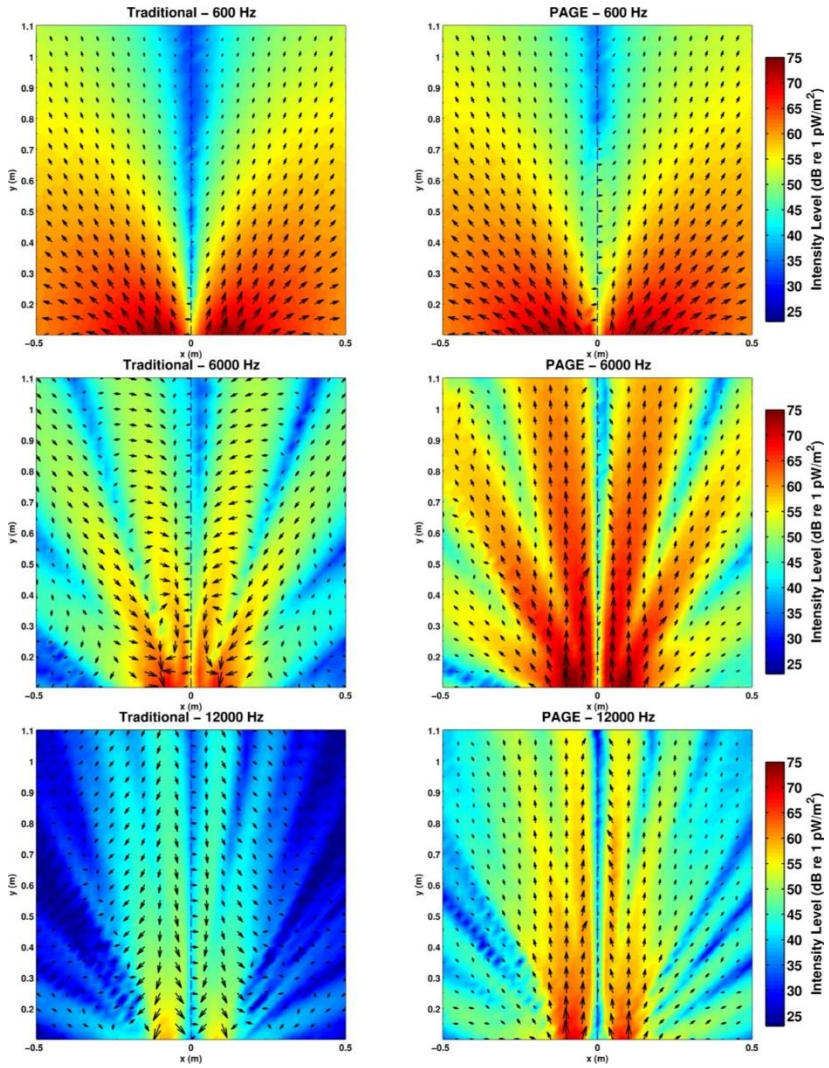

Figure 7 - *Estimates of active intensity from the traditional method (left) and PAGE method (right) at frequencies of 600 Hz (top), 6000 Hz (middle), and 12 kHz (bottom) a two-dimensional probe with radius of 5-cm measuring a two loudspeaker emitting broadband white noise 180 degrees out of phase with each other.*

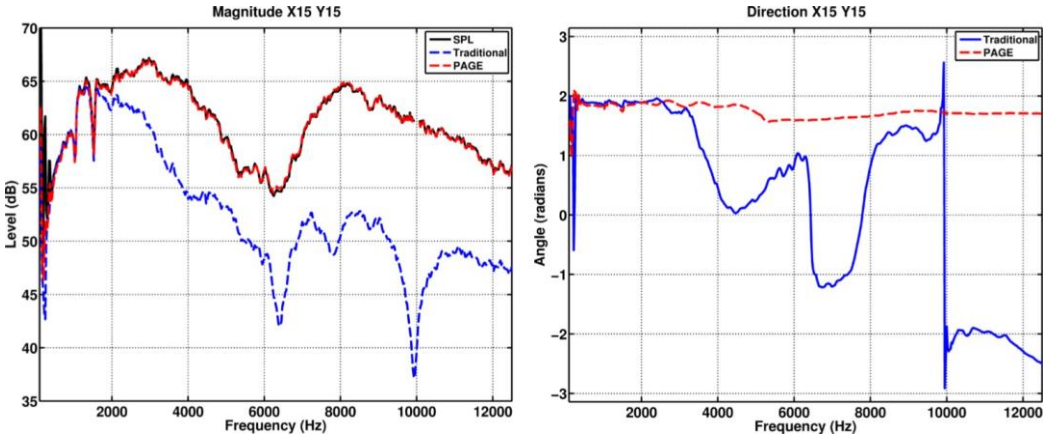

Figure 8 - *The resulting magnitude (left) and direction (right) of the intensity vector at the gird location of (15, 15) and at the spatial location, in meters, of (-0.15, 0.45) for a two loudspeakers emitting the same broadband white noise signal 180 degrees out of phase from each other. Measurements taken using a two-dimensional probe with radius of 5-cm.*

3.3 Two Incoherent Sources: Probe Radius

This set of measurements of two loudspeakers each radiating a unique broadband white noise was taken with two probes, one of radius 5.08 cm and the other with radius 2.54 cm. This source configuration lends insight into the effective bandwidth of each method without the added complexity of interference nulls caused by inter-source coherence. The corresponding intensity vector plots are displayed in Figure 9 for the 2.54 cm probe. Given the overall similarity for the 5.08 cm probe, corresponding vector maps are not shown for that probe. The intensity estimates in Figure 9 confirm the behavior of the previous measurements. At 600 Hz, the resulting field appears similar to the model in Figure 4 and is similar to that of the single source. At 12 kHz, both probe sizes perform similarly, with the PAGE providing plausible results, whereas the traditional method yields nonphysical intensity estimates. Again the 2.54 cm probe Figure 9 has the identical outcomes. Both probe sizes have results comparable to the results of the model for 2 incoherent sources at 12 kHz in Figure 4.

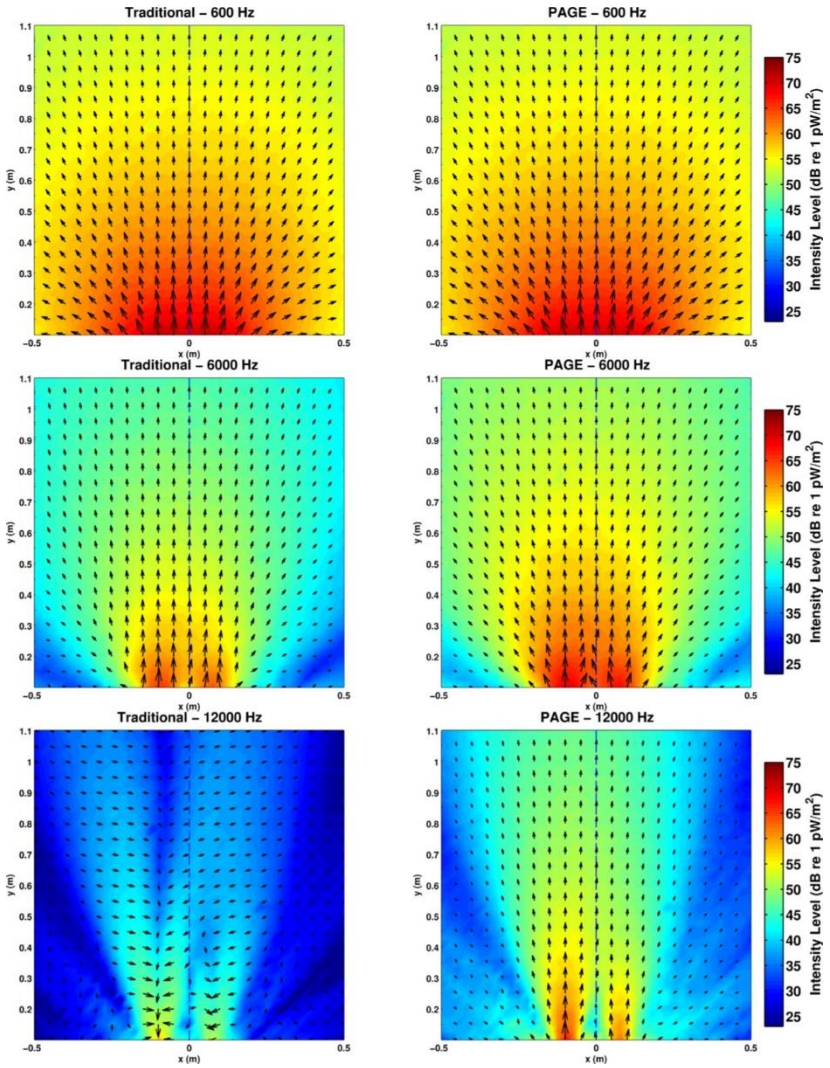

Figure 9 - *Estimates of active intensity from the traditional method (left) and PAGE method (right) at frequencies of 600 Hz (top), 6000 Hz (middle), and 12 kHz (bottom) from a two-dimensional intensity probe with radius of 2.5 cm measuring a two loudspeaker emitting broadband white noise 180 degrees out of phase with each other.*

The frequency-dependent intensity level (left) and direction (right) at location (-0.15, 0.45) are shown in Figure 10 for the 5.08 cm probe, and Figure 11 for the 2.54 cm probe. The levels show that the PAGE method follows the SPL of the center microphone very closely to beyond 12 kHz for both probe sizes. On the other hand, the traditional method's bias errors vary with probe size. The 1-dB level error in the traditional estimate is exceeded by 1.8 kHz for the 5.08 cm probe and 2.8 kHz for the 2.54 cm probe. The intensity directions are consistent between the two PAGE calculations, whereas errors become significant at 3 kHz for the 5.08 cm probe, and 6 kHz for the 2.54 cm probe.

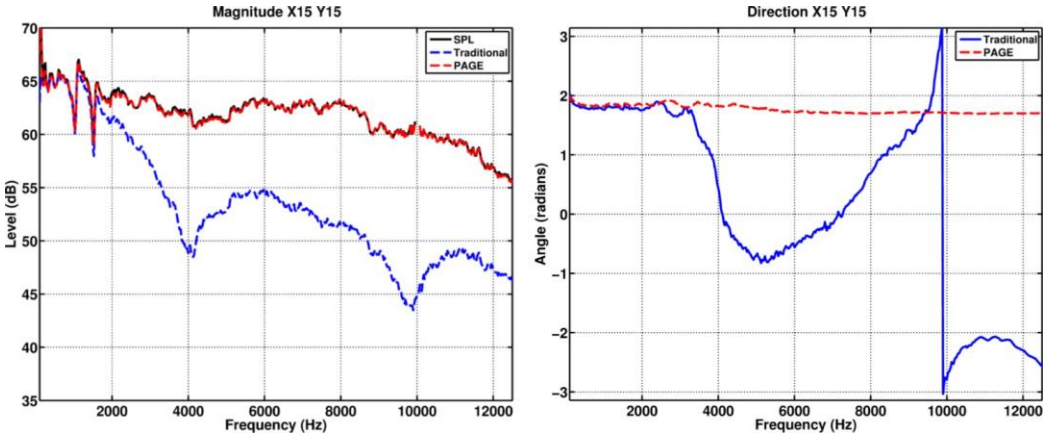

Figure 10 - *The resulting magnitude (left) and direction (right) of the intensity vector at the gird location of (15, 15) and at the spatial location, in meters, of (-0.15, 0.45) for a two loudspeakers emitting the same broadband white noise signal 180 degrees out of phase from each other. Measurements taken using a two dimensional probe with radius of 5.08 cm.*

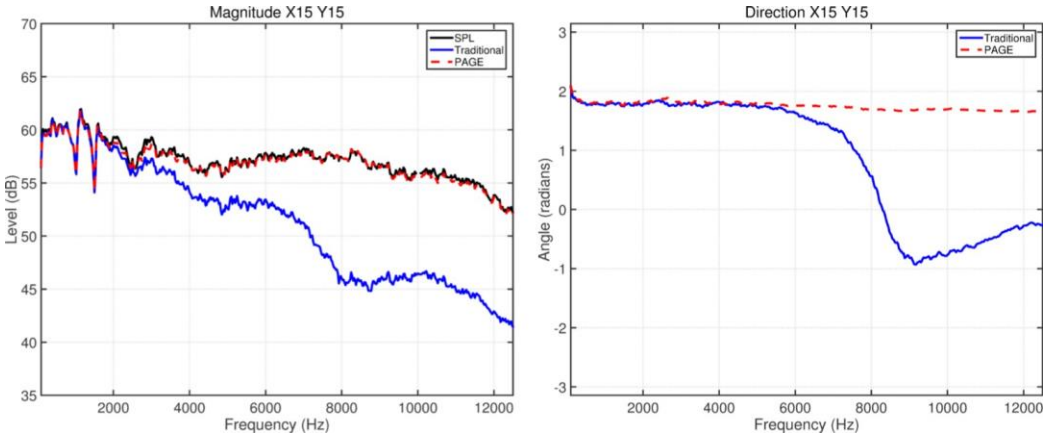

Figure 11 - *The resulting magnitude (left) and direction (right) of the intensity vector at the gird location of (15, 15) and at the spatial location, in meters, of (-0.15, 0.45) for two loudspeakers each emitting a unique broadband white noise signal. Measurements taken using a two dimensional probe with radius of 2.54 cm.*

4. CONCLUSION

The results indicate that the PAGE method does improve the frequency bandwidth of calculated acoustic vector intensity, particularly for a broadband source that permits phase unwrapping of transfer functions beyond the spatial Nyquist frequency. The results for multiple source configurations and different probe sizes suggest that the PAGE method may extend the measurement bandwidth over the traditional method several (at least 3-4) times.

With the potential of the PAGE method for improving bandwidth of intensity calculations, additional investigations are needed to evaluate its performance in different situations. This includes noise-floor estimates, the effect of probe scattering, and the effect of interference fields on the ability to unwrap the required transfer function phase.

ACKNOWLEDGMENTS

A grant from the National Science Foundation under Grant No. 1538550 supported this research.

REFERENCES

[1] Thomas, Derek C., Benjamin Y. Christensen, and Kent L. Gee. "Phase and amplitude gradient method for the estimation of acoustic vector quantities," J. Acoust. Soc. Am.**137**, 3366-3376 (2015).
[2] K. L. Gee, E. B. Whiting, T. B. Neilsen, M. M. James, and A. R. Salton, "Development of a Near-field Intensity Measurement Capability for Static Rocket Firings," Trans. JSASS Aerospace Tech. Japan **14**, No. Po_2_9-Po_2_15, (2016).
[3] T. A. Stout, K. L. Gee, T. B. Neilsen, A. T. Wall, and M. M. James, "Source characterization of full-scale jet noise using acoustic intensity," Noise Control Eng. J. **63**, 522-536 (2015).
[4] K. L. Gee, T. B. Neilsen, E. B. Whiting, D. K. Torrie, M. Akamine, K. Okamoto, S. Teramoto, and S. Tsutsumi, "Application of a Phase and Amplitude Gradient Estimator to Intensity-Based Laboratory-Scale Jet Noise Source Characterization," Berlin Beamforming Conference Paper BeBeC-2016-D3 (2016).
[5] M. J. Crocker, "Measurement of sound intensity," in Handbook of Acoustical Measurements and Noise Control, edited by C. M. Harris (McGraw-Hill, New York, 1991), pp. 14.1–14.17.
[6] J. A. Mann III and J. Tichy, "Near-field identification of vibration sources, resonant cavities, and diffraction using acoustic intensity measurements," J. Acoust. Soc. Am. **90**, 720–729 (1991).
[7] C 1043:1993, "Electroacoustics—Instruments for the measurement of sound intensity—Measurement with pairs of pressure sensing microphones" (International Electrotechnical Commission, Geneva, Switzerland, 1993).
[8]J. Y. Chung, "Cross-spectral method of measuring acoustic intensity without error caused by instrument phase mismatch," J. Acoust. Soc. Am. **64,** 1613-1616 (1978).
[9] Wiederhold, C. P., Gee, K. L., Blotter, J. D., Sommerfeldt, S. D., & Giraud, J. H. "Comparison of multimicrophone probe design and processing methods in measuring acoustic intensity," J. Acoust. Soc. Am. **135,** 2797-2807 (2014).
[10] ANSI/ASA S1.9-1996, Instruments for the Measurement of Sound Intensity (Acoustic. Soc. Am., Melville, NY, 1996).
[11] IEC 1043:1993, "Electroacoustics—Instruments for the measurement of sound intensity—Measurement with pairs of pressure sensing microphones" (International Electrotechnical Commission, Geneva, Switzerland, 1993).
[12] D. C. Thomas, B. Y. Christensen, and K. L. Gee. "Phase and amplitude gradient method for the estimation of acoustic vector quantities," J. Acoust. Soc. Am. **137**, 3366-3376 (2015).
[13] M. Akamine, K. Okamoto, K. L. Gee, T. B. Neilsen, S. Teramoto, T. Okunuki, S. Tsutsumi, "Effect of Nozzle-Plate Distance on Acoustic Phenomena from Supersonic Impinging Jet," AIAA Paper 2016-2903 (2016).
[14] F. Jacobsen, "Sound intensity measurements," in Handbook of Noise and Vibration Control, edited by M. J. Crocker (Wiley, Hoboken, NJ, 2007), pp. 534–548.
[15] J. K. Thompson and D. R. Tree. "Finite difference approximation errors in acoustic intensity measurements," J. Sound Vib. **75**, 229-238 (1981).
[16] Whiting, E. B., Gee, K. L., Sommerfeldt, S. D., & Neilsen, T. B. "A comparison of different methods for calculating complex acoustic intensity." J. Acoust. Soc. Am. **139,** 2032-2032 (2016).
[17] Whiting, Eric B. "Energy Quantity Estimation in Radiated Acoustic Fields." MS Thesis, Brigham Young University, 2016